SOME EXPERIMENTS IN CAVITATION BUBBLE DYNAMICS

Thesis by

Andrew G. Fabula

In Partial Fulfillment of the Requirements

For the Degree of

Aeronautical Engineer

California Institute of Technology

Pasadena, California

1958

ACKNOWLEDGEMENTS

The writer wishes to thank Professor M. S. Plesset for his many valuable suggestions and Dr. A. T. Ellis for loaning the timing and photographic equipment and for essential help with its adjustment.

ABSTRACT

Observations of the shape distortion during collapse of individual cavitation bubbles with maximum radii of about 0.5 to 1 cm have been made for collapse times of three to fourteen milliseconds; these observations are compared with theory. The bubbles were produced in superheated water and photographed at 3000 or 5000 frames per second. Growth was triggered by electrolysis and collapse was produced by pressurization. The distortions of bubble shape from spherical were found to be fairly well predicted by the theory of M. Rattray, when his perturbation parameter was adapted in a simple manner to the conditions used. A large variation in the collapse noise, due to bubble distortion caused by translational velocity, was observed to occur over the range of conditions tested.

TABLE OF CONTENTS

LIST OF SYMBOLS*

c_{p_g}	specific heat of hydrogen gas at constant pressure, 1.47 joule/gram ^{o}C
c_{p_v}	constant pressure specific heat of water vapor
c	specific heat of water at constant volume
d	normal distance from bubble center to surface
D	thermal diffusivity of water, i.e. thermal conductivity divided by ρc
g	gravitational constant
k	Rattray's perturbation parameter, $V_o\sqrt{\frac{p_o - p_v}{\rho}}$
L	latent heat of evaporation
m_g	mass of hydrogen gas in bubble
m_v	mass of water vapor in bubble
M	momentum of flow due to translational velocity of bubble
M_o	constant M assumed in Rattray's theory
p_g	partial pressure of hydrogen at the reference radius R_1
p_o	hydrostatic pressure at bubble center
p_v	saturated water vapor pressure for temperature T_o
dp_v/dT_o	thermal rate of variation of saturated water vapor pressure
R	bubble radius during growth and collapse
$\dot{R}$	derivative of R with respect to time
R_m	maximum radius of the bubble
R_1	a reference bubble radius

---

* Values of physical properties of water and water vapor used in calculations in this work are collected together in the List of Physical Properties of Water and Water Vapor at 25°C.

R_o, R_2, R_3	coefficients in Rattray's third-order result for bubble shape
R_o'	critical value of R_o at which appreciable bottom flattening first occurs
t	time generally measured from the start of growth or collapse
T_b	boiling point of water at pressure p_o
T_o	temperature of water in beaker
T_1	gas temperature after adiabatic compression
T_2	temperature of gas-vapor mixture
U	displacement volume of bubble
V	upward translational velocity of bubble center
V_o	initial translational velocity of bubble considered in Rattray's theory
V_o'	effective V_o due to buoyancy forces acting before and during collapse
γ	ratio of specific heats for hydrogen
Δ	vertical migration of explosion bubble during first bubble period, due to gravity alone
Δ'	vertical migration with image effect
ρ	density of water
ρ_v	density of saturated water vapor
σ	surface tension of water
τ	collapse time

LIST OF PHYSICAL PROPERTIES OF WATER AND WATER VAPOR AT 25°C*

c_{p_v}	1.86 joule/gram °C
c	4.13 joule/gram °C
D	1.5×10^{-3} cm^2/sec
L	2.44×10^{10} erg/gram
ρ_v	23.7 mm Hg
dp_v/dT_o	1.41 mm Hg/°C
ρ	0.997 gram/cm^3
ρ_v	2.3×10^{-5} gram/cm^3
σ	72 dyne/cm

---

* Taken from Dorsey, N. E., Properties of Ordinary Water Substance, Reinhold Pub. Corp., New York, (1940).

I. INTRODUCTION

As part of the growing research on cavitation, that on the dynamics of collapsing bubbles has been directed at understanding the mechanics and effects of cavitation bubble growth and collapse.* The work reported herein is a continuation of some parts of the observations of collapse dynamics given by A. T. Ellis (1). While Ellis studied the collapse of cavitation bubbles of about 0.25 to 0.5 cm maximum diameter, with collapse times of some fraction of a millisecond, the work herein is with bubbles of about 0.5 up to 1 cm maximum radius and three to fourteen milliseconds collapse time, τ. Large variations in the bubble shape distortion process occur for this range of collapse times.

The work was originally directed at study of spherical collapse which Ellis had begun with a free-fall arrangement to allow growth and collapse in a uniform pressure environment. Thus the asymmetrical shape distortions, due basically to static pressure gradient, should not occur and predicted instability of the bubble wall could be studied (2).

However in the course of work with gravity, notable collapse processes were observed, and so the major work has been with bubbles in the usual hydrostatic pressure gradient. Some findings are as follows. For the conditions tested, the observed shape distortion is predicted by the theory of M. Rattray (3). The use of his perturbation parameter, k, which is essentially translational velocity times collapse time divided by maximum bubble radius, was slightly modified

---

* For a recent survey of the literature on the dynamics of transient cavities, see Applied Mechanics Reviews, 10, 3, March 1957.

to consider varying pressure and translational momentum. When this parameter is greater than approximately 0.15 or so, translational velocity of the bubble causes it to assume a well defined spherical-cap shape, which culminates in a torus form at collapse. Qualitative observation indicates a large decrease in the collapse noise with increase in k from 0.1 to 0.4.

The possible effects of the hydrogen content of the bubbles on the bubble dynamics observed were estimated and found to be negligible over the radius range observed.

II. GENERAL DESCRIPTION OF THE EXPERIMENT

The experiments consisted of triggering the growth of a cavitation bubble in a beaker of superheated water at low pressure, allowing the bubble to grow for about twenty milliseconds and then collapsing it by rapidly increasing the pressure in the beaker. The growth and collapse was photographed at 3000 or 5000 frames per second, with a rotating-mirror camera built by A. T. Ellis (1). A flash tube* producing flashes of about a microsecond duration was used to stop the motion. With a condensing lens to concentrate the light and provide framing, suitable exposure on Eastman Tri-X film was obtained at f:14. The camera lens of 178 mm focal length gave a magnification of about 1.3. Figure 1 shows the general arrangement of beaker, camera, and the electronic equipment, and Fig. 2 shows a block diagram of the apparatus. Figure 3 is a close-up of the beaker and triggering wire. As shown by Fig. 4, which is a picture of a ruler set in the beaker, the beaker windows produced the desired linear image scale. The framing produced by the light source is indicated by the circle shown in Fig. 4.

The flash timing and producing equipment consisted of pulse generator, delay and duration timer, thyratron flash controller and various power supplies. The flash frequency was precisely adjusted by using a 1000 cycle standard oscillator and the audio oscillator to create Lissajous figures.

Since the initial purpose was to observe growth and collapse in free fall, triggering of the bubbles was convenient. Hydrogen bubble

---

* Edgerton, Germeshausen and Grier FX-2.

nuclei, produced by electrolysis at the tip of a fine enameled wire, were found suitable (see Fig. 3). Some other considerations of this method of triggering are given in later sections.

Because of the relatively low speed photography used, long collapse times were necessary to give useful details. Thus, the slow pressure rise allowed by the flexible hoses, between the beaker and the solenoid-operated valve, was not undesired. In fact, a small volume reservoir of air at atmospheric pressure was used instead of the room air. A strain-gage pressure transducer was used to obtain the beaker pressure versus time. However, the precision of this measurement was found to be only sufficient to show that the observed collapse rates were reasonably predicted by theory as shown later. A Kin-Tel D.C. amplifier, used to give sufficient voltage input to the Dumont 322-A oscilloscope, allowed static calibration of the strain gage over the pressure range covered.

Either tap or distilled water was used in the beaker. The water was partially de-aerated by causing it to cavitate acoustically at low pressure and pumping off the gases released. When so treated for an hour or so, the water would easily support several degrees of superheat at room temperature (25°C). At this temperature, each °C superheat corresponds to about 1.4 mm Hg underpressure, where underpressure is defined as saturated vapor pressure, p_v, minus local static pressure, p_o. About half an inch of vacuum-pump oil was used on top of the water to prevent evaporation (see Fig. 3). This prevented contamination of the oil in the vacuum pump, eliminated the

cause of a vertical temperature gradient in the water, and also kept the water de-aerated. Water temperature was measured before each experiment but changed only slowly with room temperature.

Portions of four typical bubble histories are reproduced in Fig. 5-7 (Bubbles No. 7, 6, 16, and 10). The image rotation between frames is a characteristic of the rotating-mirror camera. However in all these pictures, the visible portion of the trigger wire is nearly horizontal—not tilted as shown in Fig. 3! Thus it can be seen that the major bubble distortion is symmetric about the vertical axis as expected. The sequence of bubbles shows the observed range of collapse distortion behavior, from small, but still appreciable, up to dominant effects of translational velocity. When bottom concavity occurs early during collapse, i.e. at a high ratio of bubble radius to maximum radius (R/R_m), the distortion continues to grow until a "spherical-cap" form is reached. Apparently when the concave bottom meets the top surface, a torus or cored vortex ring is the form of final collapse. Perhaps the decreasing diameter of this torus, due to its formation at smaller R/R_m with decrease of translational velocity effect, is the explanation for the distinctive shapes of the bubbles after first rebound. It would have been valuable to have studied even shorter collapse times, but the maximum flash rate was the limiting factor.

Several minor effects can be noted. As seen clearly on the negatives, the growing bubble is cusped inward at the wire, but the resultant bubble shape distortion is small. During collapse, a small disturbance due to separation from the wire is occasionally seen, as

for example in Fig. 6. Occasionally slight asymmetry (other than that due to the wire) is seen in some cases during the early part of growth. Based on separate observations of the very early stages of growth, this is believed to indicate that more than one bubble grew on the tip of the wire before merger into a single bubble occurred.

Before comparing the observed collapse dynamics with theory, possible effects of hydrogen content and beaker environment on the bubble dynamics will be considered.

III. THE USE OF HYDROGEN BUBBLES AS CAVITATION NUCLEI

By generating a very small cavitation nucleus of hydrogen as in superheated water, the growth of a cavitation bubble and then its collapse due to pressurization, can be observed conveniently under controlled conditions. In common with spark generation, the method has the disadvantage of a disturbance in the neighborhood of the bubble, but only one wire is needed instead of two and no particles of wire material are thrown off to disturb the bubble surface. Most importantly, the possible gas content of the bubble and hence its effect on bubble dynamics can be accurately estimated.

Bubble growth was triggered by generating the hydrogen at the bare tip of an enameled copper wire, 0.007 inches in diameter. A 0.1 microfarad capacitor charged to 180 volts, was automatically switched from charging dry cells to the wire to create the bubble, as shown in Fig. 2.

The maximum amount of hydrogen that the capacitor charge of 18 microcoulombs can liberate is 9.4×10^{-11} grams. It is interesting to compare the charge used with the amount necessary to create hydrogen-water vapor bubbles which are in unstable equilibrium for growth for various underpressures. Using the isothermal analysis of Ref. 4, for water at 25°C, typical results are

$p_v - p_o$ (mm Hg)	0.946	1	2	3	4
Charge (microcoulombs)	18	16.11	4.03	1.79	1.001

Thus the 18 microcoulomb charge used in the experiments would not produce a sufficiently large bubble for less than about one mm Hg underpressure.

Actually the hydrogen released at the wire tip generally forms in a few small bubbles which were seen to coalesce during growth. This, plus the presence of the wire, and the changing hydrogen content complicated the actual process. However, it was frequently found that too low an underpressure would not produce growth and instead, if the beaker was not pressurized, the bubbles would be seen to rise some distance from the wire and then grow abruptly. This is reasonable since the hydrostatic pressure gradient makes the underpressure about 5 mm Hg greater at the water surface than at the wire.

A rough check on the hydrogen liberated was made using the residue bubbles in Fig. 5. For the measured static pressure at the time of Frame 73, a gas-vapor bubble, with diameter equal to that of the trigger wire (0.007 in), would contain about 3×10^{-11} grams of hydrogen. Thus, considering the lower pressure expected in the flow disturbance left at the time of Frame 73, the residue volume observed is about as expected for the predicted hydrogen liberation.

The temperature rise of the trigger wire due to the discharge current should be roughly 7×10^{-7} °C for each discharge. Thus the heating effect on the water by the wire is completely negligible.

IV. EFFECT OF HYDROGEN CONTENT ON COLLAPSE

Since the minimum cavitation bubble studied is about 0.5 cm in maximum radius, the maximum possible hydrogen content of 9.4×10^{-11} grams then produces a partial pressure of 17×10^{-4} mm Hg for water temperature, T_o, of about 25°C.

If an isothermal or adiabatic compression of the hydrogen is assumed, its partial pressure is directly determined as a function of R/R_m. For the adiabatic process, the temperature rise ratio, T_1/T_o, for compression from R_m down to some other radius, R_1 is

$$T_1/T_o = (R_m/R_1)^{3(\gamma-1)}$$

where γ is the ratio of specific heats. Thus for $R_1/R_m = 1/6$ and $\gamma = 1.41$, T_1/T_o is 8.6 and T_1 is about 2300°C! Because of the heat capacity of the water vapor in the bubble and also heat loss to the fluid, this increase cannot occur. By considering heat exchange between the gas at T_1 and only the vapor remaining in the bubble at R_1, a very conservative estimate of the maximum possible temperature increase, $T_2 - T_o$, due to the hydrogen should result. Thus for an isobaric process, one has

$$c_{p_v} m_v (T_2 - T_o) = c_{p_g} m_g (T_1 - T_2)$$

where m_v and m_g are the respective masses of vapor and hydrogen, and c_{p_v} and c_{p_g} are the respective specific heats. Since

$$m_v \geq \rho_v (T_o) (4/3)\pi (0.5)^3 (1/6)^3 \cong 5.6 \times 10^{-8} \text{ gram}$$

where $\rho_v(T_o)$ is the saturated water vapor density at T_o, one obtains for $m_g = 9.4 \times 10^{-11}$ gram,

$$T_2 - T_o < 3^{\circ}C .$$

Because heating due to condensation, as discussed next, is much greater, one concludes that the temperature of the gas and vapor is not appreciably affected directly by the gas. To the extent that the gas slows down the collapse process, less vapor is condensed, and there is more time for heat loss to the fluid. Thus the heating due to condensation is conservatively estimated by neglecting the gas. Since S. A. Zwick (6) has calculated the temperature increase in a collapsing vapor bubble for conditions nearly the same as for this work, his result of about $30^{\circ}C$ temperature rise for $R/R_m = 1/6$ is of interest.* With this temperature rise, the hydrogen's partial pressure for $R/R_m = 1/6$ is 240 times that for $R/R_m = 1$ or 0.4 mm Hg. By considering the Rayleigh equation for the bubble radius versus time, discussed in Part VI, one finds that for such a pressure increase, which is small compared with the minimum overpressure (4 mm Hg) used here, there is negligible slowing of the collapse rate until R/R_m is even smaller than 1/6.

---

* As shown in Ref. 5, for equal T_o's, the temperature increase should scale as $R_m/\sqrt{\tau}$. Thus for $R_m \leq 1$ cm and $\tau \geq 0.003$ sec, the increase should be roughly equal or less than that calculated in Ref. 6 where $T_o = 22^{\circ}C$, $R_m = 0.25$ cm, and $\tau = 0.0003$ sec are considered.

Thus the hydrogen content should not affect the collapse process in the range of R/R_m observed in this work. Obviously, however, the rebound of the bubble may be appreciably affected. Rebound was observed in all cases in this work, while as discussed in Ref. 1 there is experimental evidence of non-rebounding bubbles at least for some cases of negligible gas content. However it is interesting to speculate whether even bubbles of negligible gas content may rebound when the collapse distortion is as large as in this work, when apparently much less of the incompressible flow energy of collapse is diverted into the compression shock wave (see Part VIII).

V. EFFECTS OF BEAKER ENVIRONMENT

Since the sides and bottom surface of the beaker and the free surface of the liquid are all at about 6 cm from the bubble center, it is necessary to estimate the possible effects of this confinement on the bubble dynamics. The horizontal surfaces are considered first. The repulsion and attraction (i.e. image effects) of such surfaces for underwater explosion bubbles have been studied in detail (7, sec. 8.8). Since the internal energy of the bubble gas is found to be small compared with the total energy of the bubble, except when the bubble is small compared with its maximum size, approximate theories of bubble image effects have been derived neglecting the internal energy. Therefore these results may also be useful for cavitation bubbles. The first-order approximate theory for image effect on bubble migration due to Herring is of interest here (7, p. 340). The total upward migration of the bubble during the first oscillation, Δ', is given as that due to gravity alone, Δ, times a correction factor for the horizontal surface (either a free surface above or a rigid one below, located at distance d from the initial bubble center):

$$\Delta' = \Delta \left(1 - 0.167\, R_m^3/gd^2\tau^2\right)^* .$$

---

* Herring's result has been rewritten here in terms of the collapse time, i.e. 1/2 the bubble period, instead of overpressure. The variation in τ due to image effects has been neglected, but the effects of rigid and free surfaces are of opposite signs and negligible in the rough estimate desired here.

Here g is the gravitational constant. For both a free surface above and a rigid surface below at equal distance, the approximate theory gives just twice the single surface effect:

$$\Delta' = \Delta(1 - 0.33\, R_m^3/gd^2\tau^2) .$$

Herring's result is based on equal growth and collapse times which are characteristic of explosion bubbles. While these times are unequal in this work, the formula should be applicable as a rough approximation since most of the image effect occurs during collapse (7, p. 331). Thus for the more critical end conditions of this work, i.e.

$$R_m \cong 0.6 \text{ cm},$$

$$\tau \cong 0.003 \text{ sec},$$

and

$$d = 6 \text{ cm},$$

then

$$\frac{\Delta'}{\Delta} \cong 1 - 0.2 = 0.8 .$$

An experimental check on this possible image effect on vertical displacement was made. The displacement of bubble center relative to the trigger wire, as for example in Frame No. 70 for Bubble No. 6 (Fig. 6), was compared with that calculated by integration of translational velocity due to buoyancy.* No noticeable differences could be measured,

---

* The calculation of this velocity, V, is essentially as discussed for the "effective initial translational velocity", V_o', in Part VII, except that

$$V = V_o'(R_m/R)^3 .$$

indicating negligible effect of both image effect and momentum decrease due to viscous effects as long as the bubbles remained approximately spherical.

Similar estimates of the effect of the beaker sidewall have not been possible. The beaker sidewall is nearly symmetric about the vertical axis through the bubble, and so no direct translational velocity effects are expected, but the side constraints might retard the growth and collapse processes. For the typical bubble maximum diameter of this work (1.5 cm), the ratio of beaker diameter to bubble diameter is 11.5: 1.5 = 7.7: 1. Ellis did not detect any effects when the beaker-to-bubble ratio was changed from 10:1 to 20:1 (1). Since the slower collapse times used in this work should reduce the image effect, the lower beaker-to-bubble ratio is not thought to be significant. For example, Fig. 8 gives typical experimental data for bubble radius, read from the films, and beaker pressure read from the oscilloscope traces for the strain-gage transducer. Using the indicated pressure versus time for Bubble No. 10, the isothermal bubble equation discussed in Part VI was integrated numerically to obtain the predicted collapse curve shown by the dashed curve. While the slower experimental collapse could be due to sidewall constraint, inaccuracy of the pressure data is felt to be the most likely cause.

VI. COMPARISON OF OBSERVED GROWTH WITH THEORY

The extended portions of nearly linear growth seen in Fig. 8 suggest an approximately isothermal bubble condition (8). As shown in Ref. 8, if the temperature of the water is appreciably lower than 100°C, say 15°C, the greatly reduced water vapor density makes negligible the cooling effect of the evaporation from the bubble wall. Thus the asymptotic isothermal growth (linear law) can occur when otherwise the asymptotic cooling effect produces a square-root law of growth. While saturated water vapor density at 25°C is about twice that at 15°C, it still is very small compared with that for 100°C. However, as discussed below, the observed growth curves do indicate the beginning of cooling effect, in agreement with approximate calculations of bubble temperature decrease.

For the exactly isothermal case, the extended Rayleigh equation for the bubble radius is (8)

$$R\ddot{R} + \frac{3}{2}\dot{R}^2 = \frac{p_v + p_g (R_1/R)^3 - p_o}{\rho} - \frac{2\sigma}{\rho R} \quad .$$

Here p_g is the pressure of the hydrogen content at a reference radius R_1; σ is the surface tension; and ρ is the water density. The equation can be rewritten as

$$\frac{1}{2R^2} \frac{d}{dR}(R^3 \dot{R}^2) = \frac{p_v - p_o}{\rho} + \frac{p_g}{\rho} \left(\frac{R_1}{R}\right)^3 - \frac{2\sigma}{\rho R} \quad .$$

and so integration gives

$$\dot{R}^2 = \dot{R}_1^2 \left(\frac{R_1}{R}\right)^3 + \frac{2}{3}\left(\frac{p_v - p_o}{\rho}\right)\left[1 - \left(\frac{R_1}{R}\right)^3\right] + \frac{p_g}{\rho}\left(\frac{R_1}{R}\right)^3 \ell n \left(\frac{R}{R_1}\right)^2 - \frac{2\sigma}{\rho R}\left[1 - \left(\frac{R_1}{R}\right)^2\right].$$

To estimate the relative magnitude of the various terms, R_1 and p_g were estimated by considering as the cavitation nucleus the minimum size gas-vapor bubble unstable to growth for 2 mm Hg underpressure, which is about the lowest underpressure used. Thus

$$R_1 = \frac{4}{3}\frac{\sigma}{p_v - p_o} = 0.036 \text{ cm}$$

and

$$p_g = (p_v - p_o)/2 = 1 \text{ mm Hg}.$$

If these and a very conservative estimate of $\dot{R}_1$, viz. 12 cm/sec (based on the discharge rate of the capacitor), are used in the isothermal relation, then for R greater than 1 mm, the equation, to an accuracy of a few percent, reduces to

$$\dot{R}^2 = \frac{2}{3}\left(\frac{p_v - p_o}{\rho}\right) - \frac{2\sigma}{\rho R}\left[1 - \left(\frac{R_1}{R}\right)^2\right].$$

Since $2\sigma/R$ is about 0.8 mm Hg for R = 1 mm, noticeably nonlinear growth, with $\dot{R}$ increasing with time, should occur for an underpressure

of 2 mm Hg. (While the $(R_1/R)^2$ term retained might be as high as 0.13, this last remaining effect of nucleus size only slightly reduces the effect of σ .) Only minute evidence of increase of $\dot{R}$ during growth can be seen in the growth curves, and actually noticeable decrease occurs well before the start of pressure rise. That this corresponds to appreciable cooling can be seen as follows. As shown in Ref. 5, the order of magnitude of bubble temperature decrease during growth is

$$\Delta T \approx - \frac{R}{3\sqrt{Dt}} \frac{\rho_v L}{\rho c} \quad .$$

Here D is the thermal diffusivity of water, equal to the thermal conductivity divided by ρc, with c the specific heat of water at constant volume.* t is the time of growth up to the radius R considered, and L is the latent heat of evaporation. In the absence of large cooling effect, the isothermal asymptotic growth law gives, for small superheats:

$$R \cong t\sqrt{\frac{2}{3\rho} (dp_v/dT_o) (T_o - T_b)} \quad ,$$

where T_o and T_b are the boiling temperatures corresponding to p_v and p_o respectively, so that $T_o - T_b$ is the superheat. Thus the temperature change can be written as

$$\Delta T \approx - \sqrt{t(T_o - T_b)} \quad \frac{1}{3}\sqrt{\frac{2}{3} \frac{dp_v/dT_o}{\rho D}} \frac{\rho_v L}{\rho c}$$

---

* The usual subscript v is omitted to prevent confusion with any vapor property.

so that for t in sec and $T_o - T_b$ in ^oC,

$$\Delta T\ (^oC) \approx -\ 4.2 \sqrt{t(T_o - T_b)}\ .$$

The approximate range of superheats for the curves in Fig. 8 is 1.5 to 2^oC. (Greater superheats made the bubbles too large compared with the beaker.) The corresponding order of magnitude approximation for ΔT at $t = 0.018$ sec (just before the start of pressure rise) is 0.7 to $0.8\ ^oC$. Thus significant cooling, corresponding to as much as 45 percent reduction in effective superheat, is indicated.

VII. COMPARISON OF BUBBLE SHAPE DISTORTION DURING COLLAPSE WITH THEORY

The observed distortion of the bubbles from spherical shape during collapse can be described as proceeding from spherical to oblate spherical, and then the bottom becoming flatter and later concave. The concavity of the bottom apparently may increase until the central portion of the bottom reaches the top, so that a final torus form is suggested. As shown below, Rattray's result predicts the observed collapse distortion as well as can be expected of perturbation theory (3).

In his study of perturbation effects in bubble dynamics, Rattray considered, besides other problems, the free-surface potential flow of a single collapsing cavitation bubble with initial translational velocity. The liquid at infinity is under uniform and constant pressure. The bubble is initially spherical with unit radius. Surface tension is omitted since its effects should be negligible for conditions of interest.

Rattray's solution gives the bubble profile R/R_m in the expansion

$$R(\theta, t)/R_m = R_o(t) + R_2 k^2 P_2(\cos\theta) + R_3 k^3 P_3(\cos\theta) + O(k^4)^* .$$

Here θ is the polar angle measured from the rearward portion of the line of motion. R_o is the θ-independent term, decreasing from 1 during collapse; R_2 and R_3 are functions of R_o; and $P_2(\cos\theta)$ and

---

* The R_1 term has been made zero by proper choice of the moving origin of the R and θ coordinate system. R_2 and R_3 correspond to $R_2^{(2)}$ and $R_3^{(3)}$ as used by Rattray.

$P_3(\cos\theta)$ are the usual Legendre polynomials. k is the small perturbation parameter defined as

$$k = V_o \sqrt{\frac{p_o - p_v}{\rho}}$$

where V_o is the initial translational velocity of the bubble, so that

$$V_o = M_o/\rho \ \frac{2}{3}\pi R_m^3$$

where M_o is the momentum of the flow. (Note that the 1/2 value for the added mass coefficient of a sphere has been used since an initially spherical shape is assumed.) This momentum is constant because the bubble contents have negligible mass; because no hydrostatic pressure gradient is considered; and because there are no other disturbances in the unbounded liquid.

Rattray used numerical integration to calculate R_2 and R_3 as functions of R_o and obtained

R_o	R_2	R_3
1.0	0	0
0.9	-0.248	-0.235
0.8	-0.588	-0.840
0.7	-1.068	-2.021
0.6	-1.778	-4.353
0.5	-2.901	-9.100
0.4	-4.861	-21.05
0.3	-8.973	-57.92
0.2	-20.37	-250
0.1	-92.75	-1000

Since the volume of the perturbed bubble can be shown to be

$$(4/3)\pi R_o^3 + O(k^4),$$

the time scale of the collapse process can be calculated from

$$t(R_o) = \int_{R_o}^{1} (R_o)^{-1} \, dR_o .$$

Rattray's solution for R_o yields

$$t(R_o) = \sqrt{\frac{3\rho}{2(p_o - p_v)}} \left[\int_{R_o}^{1} \frac{R_o^{3/2}}{\sqrt{1 - R_o^3}} \, dR_o + \frac{k^2}{8} \int_{R_o}^{1} \frac{R_o^{-3/2}}{\sqrt{1 - R_o^3}} \, dR_o + O(k^4) \right]$$

The first integral is the well-known Rayleigh integral (10). For this work the second integral was calculated approximately by a numerical procedure. Typical values are given in the following table.

R_o	$\int_{R_o}^{1} \frac{R_o^{-3/2}}{\sqrt{1 - R_o^3}} \, dR_o$
1	0
0.9	0.393
0.8	0.601
0.6	1.030
0.4	1.649
0.2	2.074
0.08	5.55

While the integral is divergent for $R_o \rightarrow 0$, its contribution to t, reduced by $k^2/8$, is only about 6 percent for k as high as 0.4 and R_o as low as 0.2. Thus negligible distortion in the time scale of collapse is indicated for the conditions of this work. The possible lengthening of collapse time for R/R_m less than 0.2 is not considered here, because of the effects not considered in Rattray's theory which become important.

Instead of trying to enlarge Rattray's work to consider varying k, the observed bubble shapes have been compared with those predicted by Rattray's result for k's chosen as follows. Since the collapse time should be negligibly affected by the shape distortion, k may be redefined by using the Rayleigh collapse time relation,

$$\tau = 0.914\, R_m \sqrt{\frac{p_o - p_v}{\rho}}$$

so that

$$k = \frac{V_o \tau}{0.914 R_m} = 1.1 \frac{V_o \tau}{R_m} .$$

First, therefore, instead of considering the changing overpressure during collapse for these experiments, the observed τ and R_m were used to determine k. This amounts to assuming the particular constant overpressure which would give the same collapse time. For the flow considered by Rattray, V_o is determined by the constant flow momentum, but this momentum can vary greatly during slow collapse in this work due to buoyancy. Second, therefore, a varying effective

initial translational velocity, V'_o, was calculated from the integral of the buoyancy force to determine the momentum acquired up to the time of interest.* Thus

$$V'_o = M(t)/\rho \frac{2}{3} \pi R_m^3$$

where

$$M(t) = \int_0^t \rho g U dt$$

for U the bubble volume and t the time from start of growth.

A comparison of predicted with observed shapes is given in Fig. 9 for two cases of major and extreme distortion (Bubbles No. 16 and 10). (Cases of small distortion are considered below.) The k value for Bubble No. 10 is so large (nearly 0.4) that this is an unfair test of Rattray's result in which terms of higher than third order have been neglected. Probably the retention of higher order terms and possibly surface tension would appreciably improve the agreement for the smaller R/R_m case for Bubble No. 16 also. A fairer comparison of theory with experiment is made by considering only distortion up to the point of noticeable flattening of the bubble bottom. This is given in Fig. 10 where the solid curve gives R'_o versus k from Rattray's result for an essentially flat bottom over the polar angle interval of 0^o to $+30^o$. The circled points mark the corresponding values at which noticeable flattening was first observed for the bubbles indicated. For

---

* Image and viscous effects are negligible, as discussed in Part V.

example, the point for Bubble No. 10 corresponds to Frame No. 59 in Fig. 6. It is reasonable that the experimental points lie below the theoretical curve because the lower k during the earlier part of collapse means less distortion than would occur during the same time if k were constant at a higher value.

It is important to note that if the restrictions of Rattray's result to negligible image effects (such as nearby boundaries or other bubbles) and initially spherical shape are not met, greatly different collapse distortion can occur. Figures 11 and 12 show cases in point. The former shows an example of large image effect observed in a preliminary free-fall test. Two extra bubbles were triggered at scratches on the wire. The pictures show how the center bubble necked down and was split in two when pulled in opposite directions by the two outer bubbles. Figure 12 taken from Ref. 1 shows the "collar-button" distortion which Ellis observed when random bubbles in boiling water were collapsed. Ellis attributes this to non-spherical shape at the start of collapse.*

---

* Private communication.

VIII. OBSERVATIONS OF NOISE DUE TO COLLAPSE

The following observation was made repeatedly during the bubble experiments. When rapid pressurization was used to collapse a bubble, so that a teardrop rebound was observed, a distinct "clink" of the beaker would be heard, undoubtedly due to collapse. In one case when unusually high underpressure and rapid pressurization were used, the beaker windows were cracked off. On the other hand, whenever the flat-topped rebound bubbles were observed, a muted clink or none at all was noticed.

In view of this evidence for a large decrease of noise radiated for k varying from 0.1 to 0.4, it is interesting to see if there is any confirming experimental data on single bubble noise due to collapse. Most of this work has been done with spark bubbles at atmospheric pressure. Since experiment (11) has shown that such bubbles grow and collapse roughly in accord with the Rayleigh formula, simple integration of the buoyant force gives the total momentum acquired during growth and collapse. The result is

$$M \cong 0.9\,(\rho g\,\tfrac{4}{3}\pi R_m^3)R_m\sqrt{\frac{3\rho}{2(p_o - p_v)}}\quad .$$

Because most of the distortion occurs late in collapse for k = 0.1, the effective initial translational velocity, V_o', is determined by this momentum so that

$$V_o' \cong 1.8\,gR_m\sqrt{\frac{3\rho}{2(p_o - p_v)}}$$

and

$$k \cong \frac{2.2\rho g R_m}{p_o - p_v} \quad .$$

Therefore, at room temperature and normal atmospheric pressure,

$$k \cong 0.002 R_m$$

for R_m in cm. Thus for $k = 0.1$, $R_m = 50$ cm — corresponding to an explosion rather than a spark!

Thus only spark experiments at reduced pressures (for room temperatures) will give the longer collapse times required to produce $k = 0.1$ or higher. While such spark experiments have been made in modeling underwater explosions, no pertinent collapse noise data was found in the literature by the writer.

The spark bubbles produced by R. H. Mellen for his noise measurements at atmospheric pressure were from 0.5 to 2.5 cm in radius (11). It is interesting that for this small range of k (0.001 to 0.005), Mellen found a 3/2-power relation between peak pressure and bubble radius. Some related work was done by M. Harrison who studied cavitation bubbles growing and collapsing in the flow through a Venturi nozzle (12). After isolating the effect of gas content on collapse noise, he found a drop-off from the 3/2 power law for his larger bubbles. It is interesting that for these bubbles of about 1 cm diameter, Harrison's pictures suggest spherical-cap collapse. Thus it seems probable that significant translational velocity was produced by the steep static pressure gradients along the nozzle. However, because of lack of data, the k's for Harrison's experiments could not

be estimated.

All the bubbles studied here were triggered by the same condenser with the same charge. Some slight variation in bubble gas content might have occurred due to variation in the time until the bare tip of the trigger wire was swallowed up in the bubble. However it seems clear that the observed variation of collapse noise with k would also occur for bubbles with negligible gas content.

Since cavitation noise due to bubble collapse is related to the secondary pulses produced by explosion bubble oscillations, one naturally wonders whether spherical-cap distortion plays an important part in determining secondary pulse strength. There seems to be little in the literature in this connection. The effect of translational velocity on secondary pulse strength has been considered only as it affects minimum bubble size, assuming spherical shape (7, Chapter 9). However, at least the early stages of spherical-cap distortion have been observed and predicted theoretically for large charges (7 and 13).

IX. CONCLUSIONS

An experimental study was made of shape distortion during collapse of single cavitation bubbles. The ranges of 0.5 to 1 cm maximum radius and total times for growth and collapse of twenty to thirty milliseconds were studied. There were no appreciable effects of the boundary surfaces and no noticeable distortion from spherical shape of the bubbles at the start of collapse. For these conditions, the early stages of shape distortion and the large dependence of the rate of distortion on bubble translational velocity were found to be correctly predicted by the perturbation theory of M. Rattray. In the observed range of 0.1 to 0.4 of Rattray's parameter, k, distortion during collapse varies from small to extreme, with the bubble assuming a spherical-cap shape and apparently collapsing to a torus of larger relative size for the larger k values. According to qualitative observation, the noise due to collapse decreases by an order of magnitude from $k = 0.1$ to 0.4.

REFERENCES

1. Ellis, A. T., "Observations on Cavitation Bubble Collapse", C.I.T. Hydro Lab. Report No. 21-12, (December 1952).

2. Plesset, M. S. and Mitchell, T. P., "On the Stability of the Spherical Shape of a Vapour Cavity in a Liquid", C.I.T. Hydro Lab. Report No. 26-9, (July 1954).

3. Rattray, M., Jr., "Perturbation Effects in Bubble Dynamics", Ph.D. Thesis, C.I.T., (1951).

4. Dergarabedian, P., "Observations on Bubble Growths in Various Superheated Liquids", Naval Ordnance Test Station NAVORD Report 5009 (NOTS 1345), (January 1956).

5. Plesset, M. S., "The Dynamics of Cavitation Bubbles", J. Appl. Mech., (September 1949), pp. 277-282.

6. Zwick, S. A., "The Growth and Collapse of Vapor Bubbles", C.I.T. Hydro Lab. Report No. 21-19, (December 1954).

7. Cole, R. H., Underwater Explosions, Princeton University Press, Princeton, N.J., (1948).

8. Plesset, M. S., "Physical Effects in Cavitation and Boiling", Symposium on Naval Hydrodynamics, Washington, D. C., (September 1956).

9. Kolodner, I. I., "Underwater Explosion Bubbles IV. Summary of Results and Numerical Computations", New York University IMM-NYU 233, (July 1956).

10. Lord Rayleigh, "Pressure Developed in a Liquid During the Collapse of a Spherical Cavity", Phil. Mag., 34, (1917), pp. 94-98; also Collected Papers, 6, pp. 504-507.

11. Mellen, R. H., "An Experimental Study of the Collapse of a Spherical Cavity in Water", J. Acoust. Soc. America, 28, 3, (May 1956), pp. 447-454.

12. Harrison, M., "An Experimental Study of Single Bubble Cavitation Noise", Taylor Model Basin Report 815, (November 1952).

13. Kolodner, I. I. and Keller, J. B., "Underwater Explosion Bubbles II. The Effect of Gravity and the Change of Shape", New York University IMM-NYU 197, (June 1953).

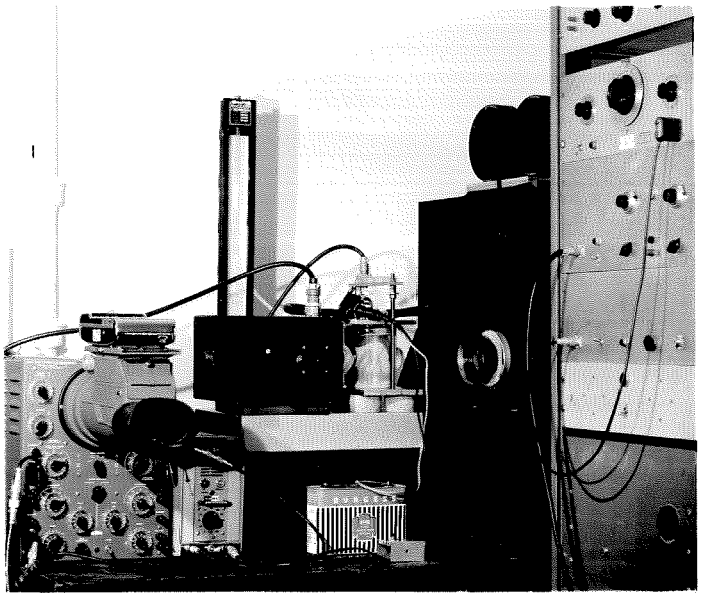

Fig. 1. General arrangement of timing and photographic equipment.

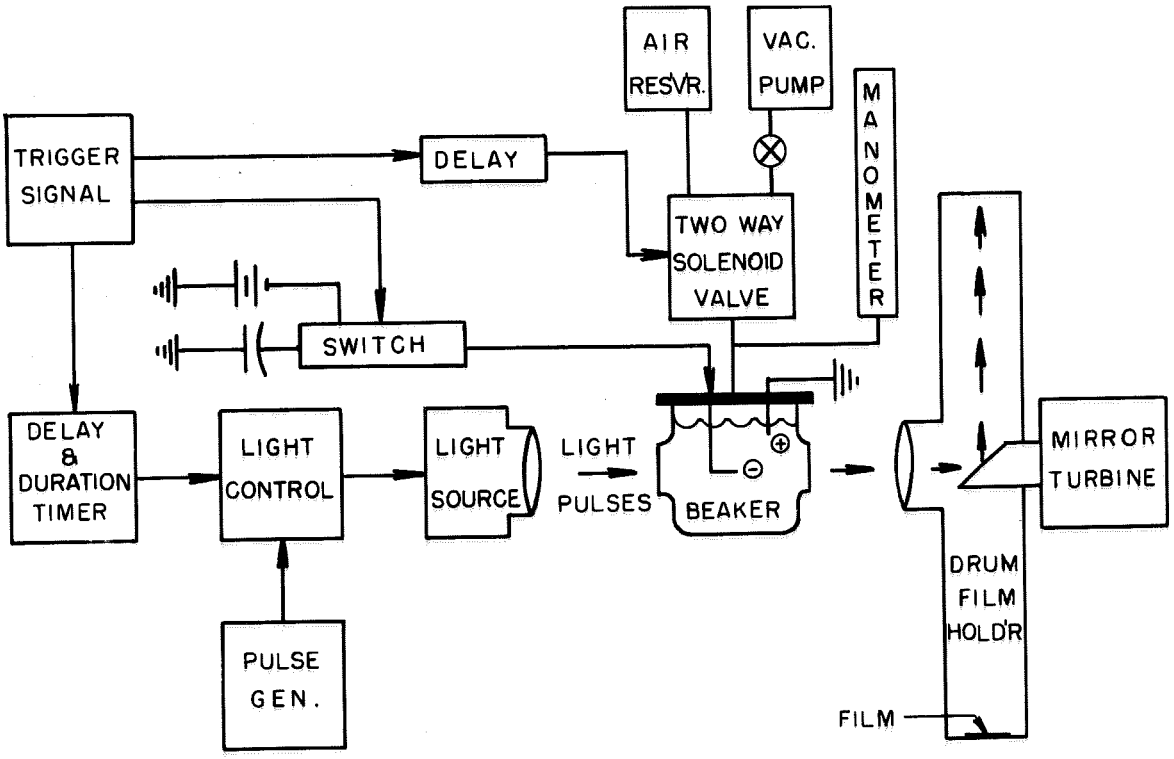

Fig. 2. Block diagram of timing and photographic equipment.

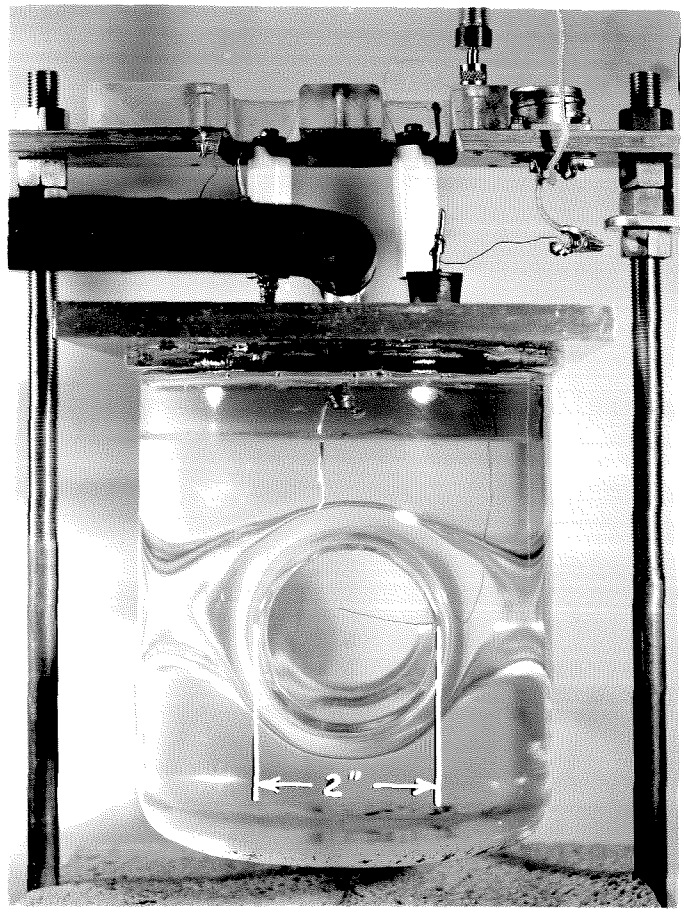

Fig. 3. Picture of beaker showing window and trigger wire. In the free-fall arrangement shown, a soft metal strip supports the beaker. Cutting this strip releases the beaker and triggers the bubble.

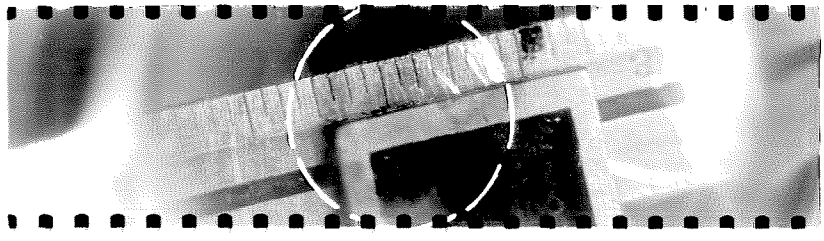

Fig. 4. Test photograph with rotating-mirror camera of a ruler set in the beaker. The circle indicates the usual framing.

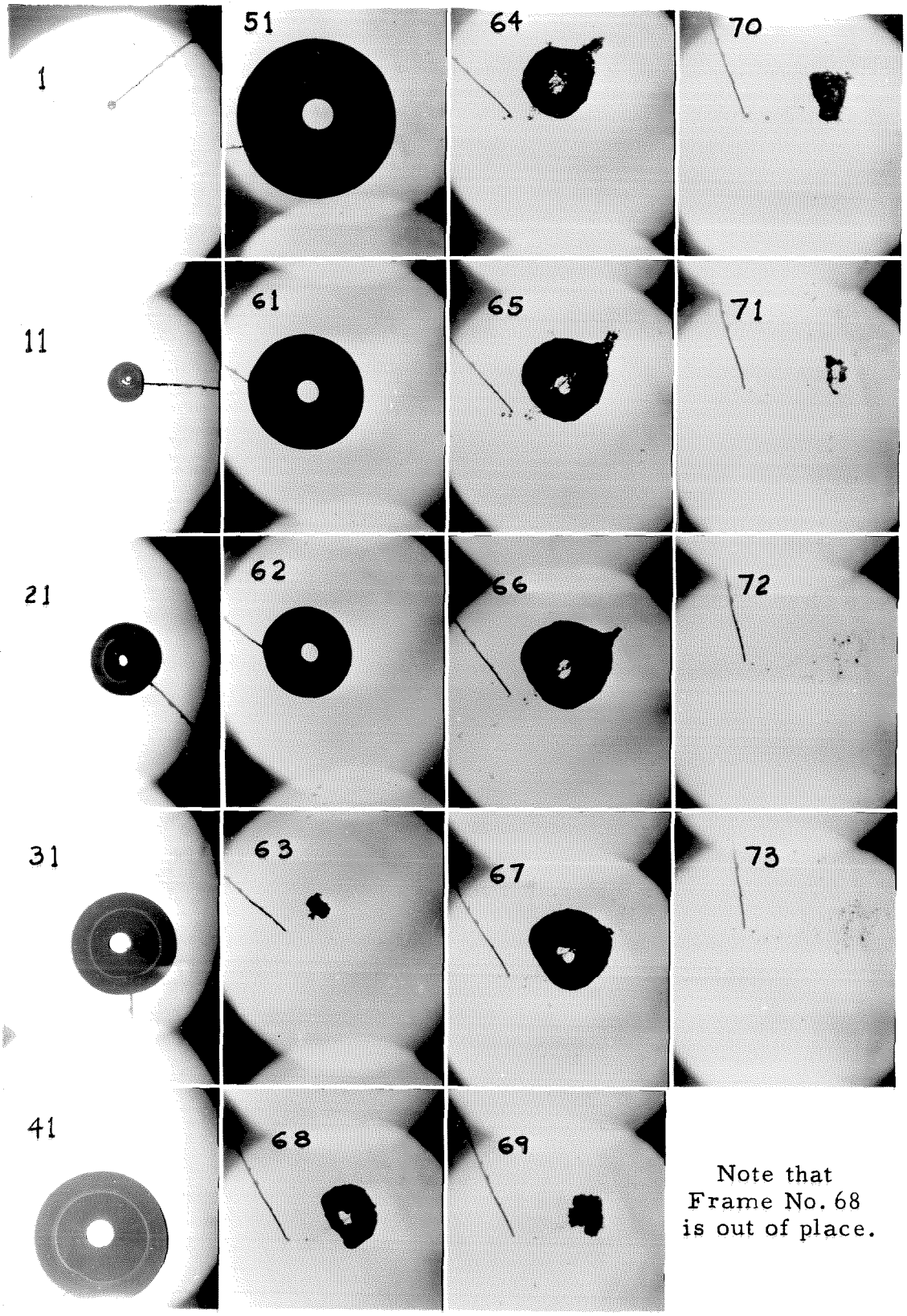

Fig. 5. Bubble No. 7; 3000 frames/sec; magnification 2.2 .

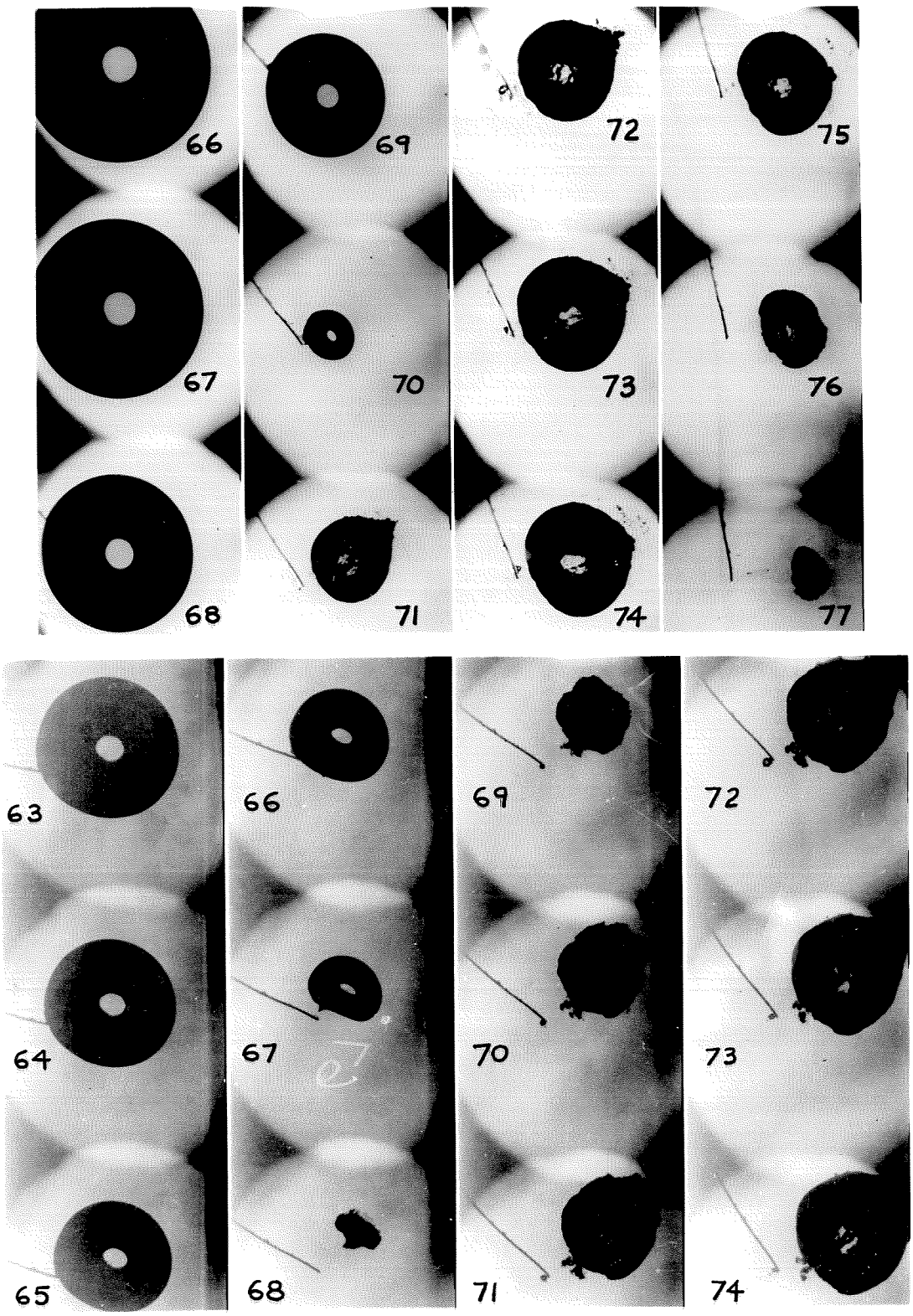

Fig. 6. Bubbles No. 6 (top) and 16 (bottom); 3000 and 5000 frames/sec respectively; magnification 1.8 and 2.1 respectively.

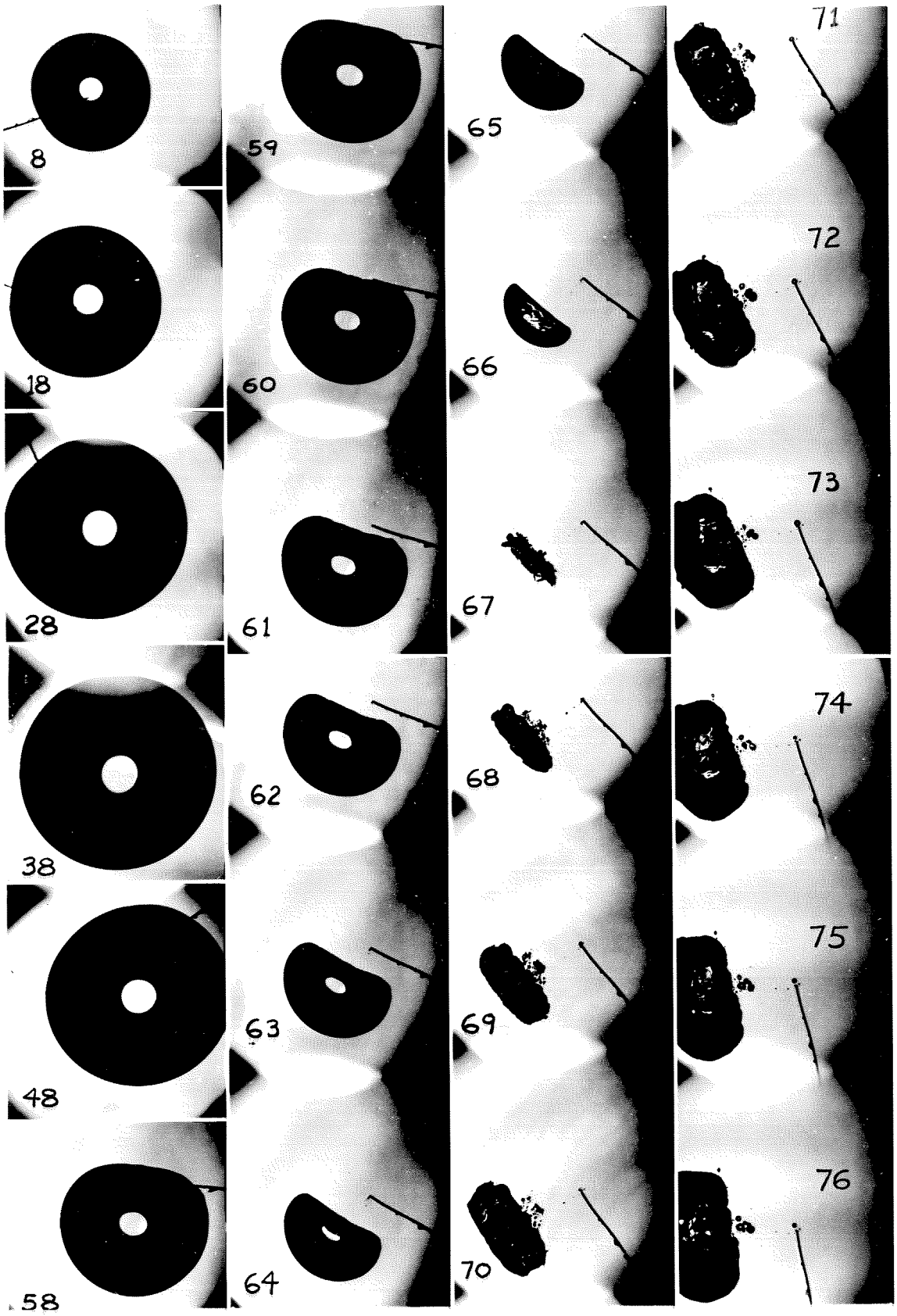

Fig. 7. Bubble No. 10; 3000 frames/sec; magnification 2.2 .

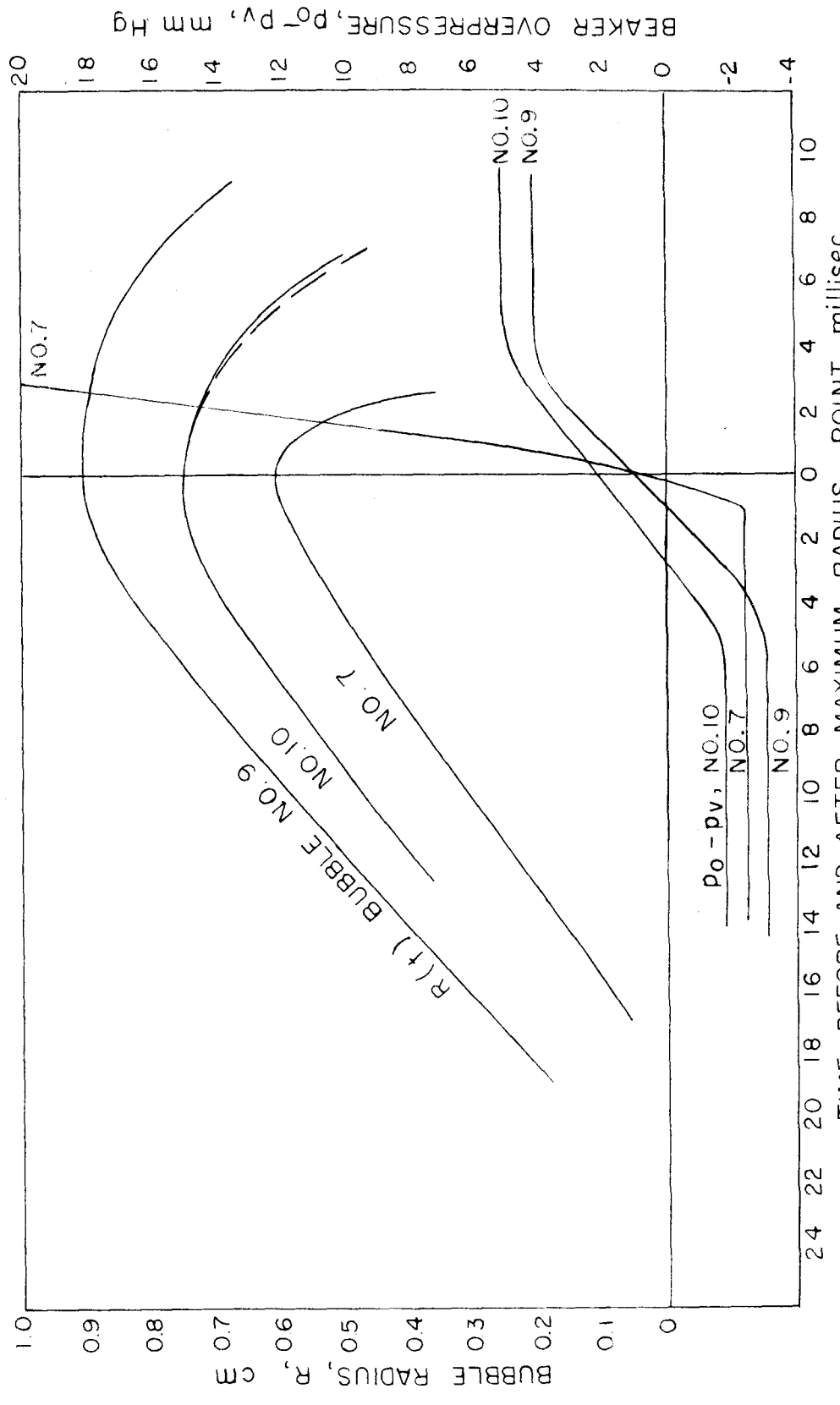

Fig. 8. Typical data for bubble radius and beaker pressure versus time.

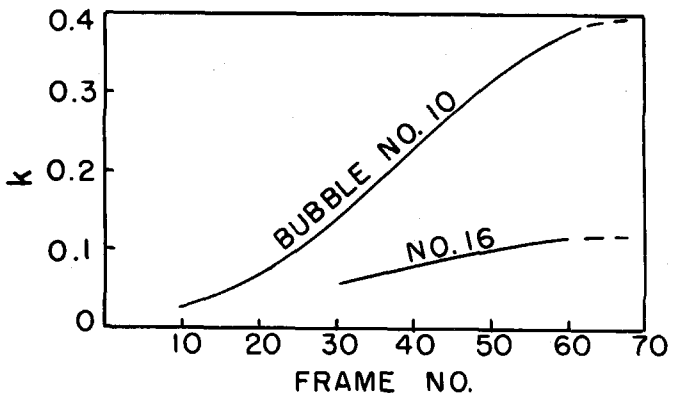

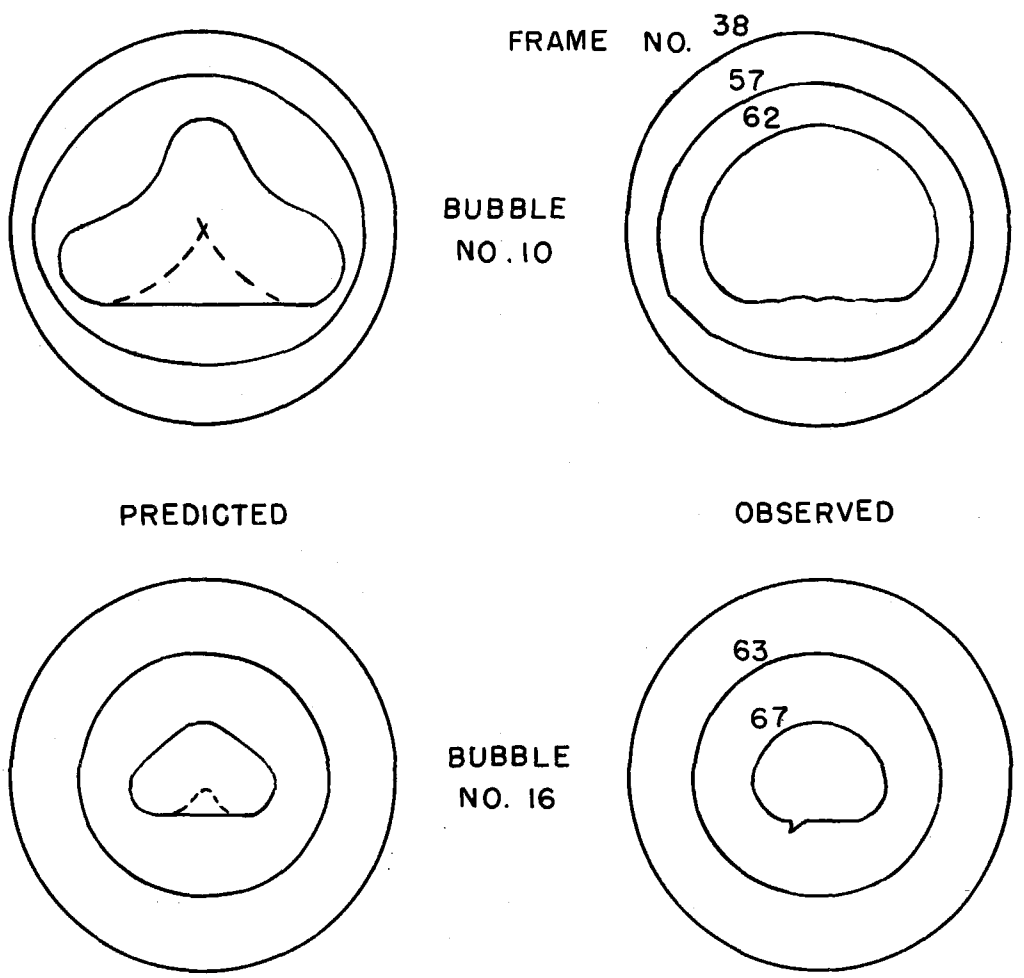

Fig. 9. Comparison of observed shapes for Bubbles No. 10 and 16 with predicted shapes for calculated k values.

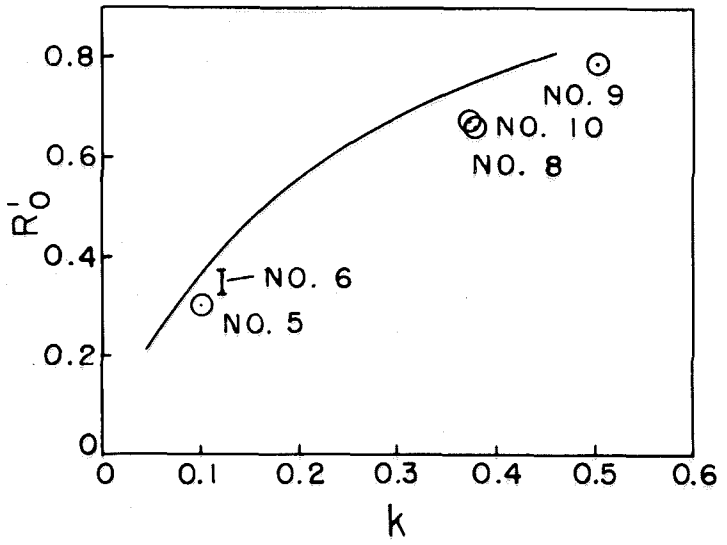

Fig. 10. Comparison of predicted and observed points of first appreciable flatness of bubble bottom surface.

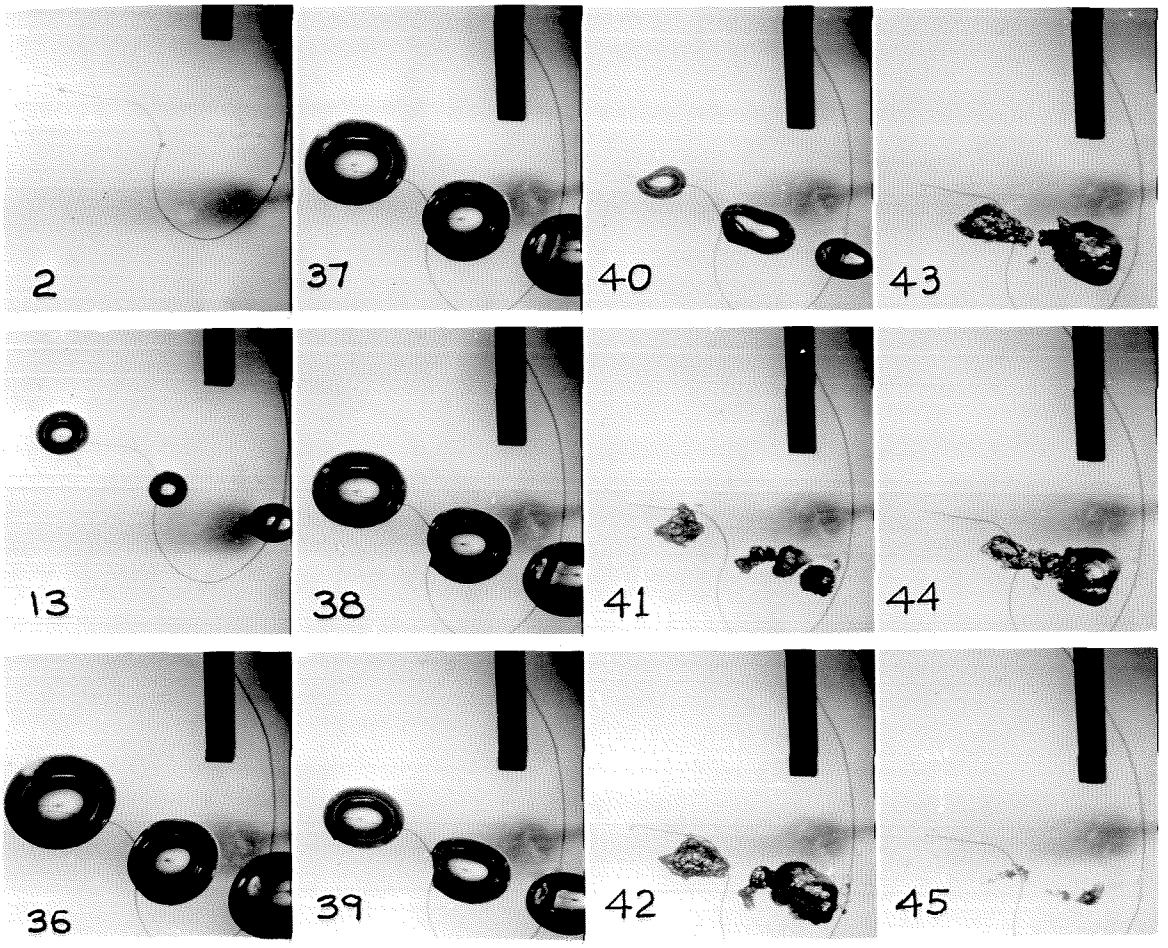

Fig. 11. Free-fall test showing large image effects, produced by the collapse of adjacent bubbles; about 2000 frames/sec.

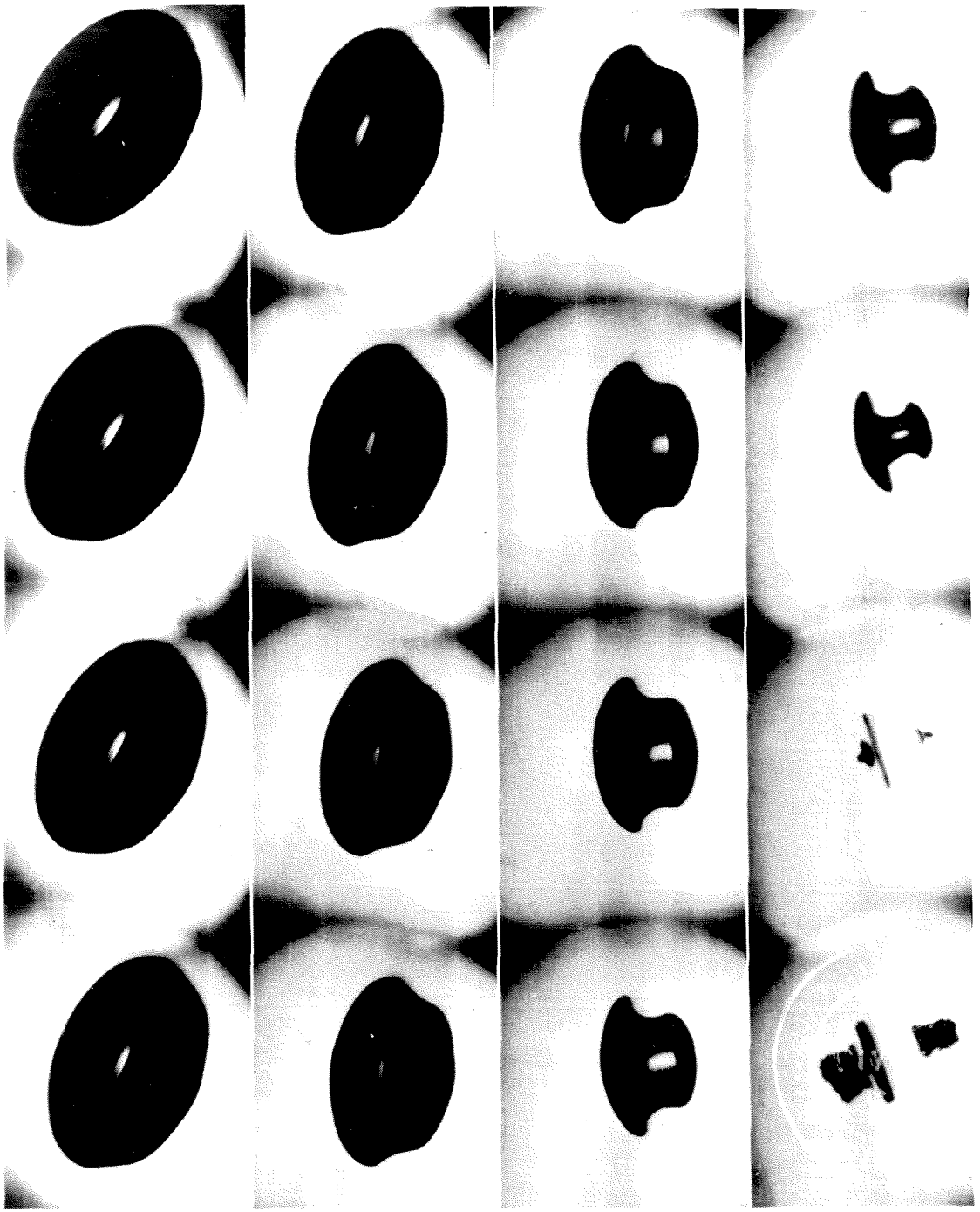

Fig. 12. Example of collar-button mode of collapse distortion, reproduced from Ref. 1; 33,000 frames/sec; magnification about 7.2.